Catalysis Science & Technology

ROYAL SOCIETY OF CHEMISTRY

COMMUNICATION

View Article Online
View Journal | View Issue

Check for updates

Cite this: *Catal. Sci. Technol.*, 2021, 11, 6649

Received 20th August 2021,
Accepted 17th September 2021

DOI: 10.1039/d1cy01518d

rsc.li/catalysis

Superior CNT-supported bimetallic RuCu catalyst for the highly selective hydrogenolysis of glycerol to 1,2-propanediol†

Magdy Sherbi,[a] Anne Wesner,[a] Valea Kim Wisniewski, [b] Anna Bukowski,[a] Hristiana Velichkova, [b] Bodo Fiedler[b] and Jakob Albert *[a]

Selective hydrogenation of glycerol to 1,2-propanediol (1,2-PD) is a promising route for sustainable production of platform chemicals. Herein, a bimetallic RuCu catalyst supported on multiwall carbon nanotubes (RuCu/MWCNT) is reported that shows superior catalytic performance leading to 93.4% 1,2-PD selectivity under mild reactions conditions.

To this date, the production of platform chemicals relies primarily on fossil resources. However, the increasing scarcity and negative environmental impact, that the use of fossil resources entails, show that the development of more sustainable production pathways is of paramount importance.[1]

Glycerol (GL) is a major by-product of biodiesel manufacturing produced in an amount corresponding to around 10 wt% of the biodiesel production. Several catalytic transformations of GL into value-added chemicals have been reported including steam reforming, oxidation, dehydration, acetylation, esterification, etherification, carboxylation and chlorination.[2–4] Nevertheless, hydrogenolysis of GL into propanediols (PDs) is one of the most attractive approaches for GL valorisation due to the wide applicability of PDs on a large scale.[5] 1,2-Propanediol (1,2-PD), or propylene glycol, is an important chemical extensively used as a monomer for polyester resin. Other industrial applications are found in the food-, pharmaceutical-, cosmetic- and animal feed industries.[6–8] Selective catalytic hydrogenolysis of GL provides an attractive, greener alternative to the current fossil-based manufacturing process of 1,2-PD.[9]

Hydrogenolysis of GL can be regarded as a two-step process involving acid-catalysed GL dehydration affording a double bond, which is then selectively hydrogenated to yield the desired PD. The acidity of the applied catalyst effects the position of remaining hydroxyl groups on PD. Several heterogeneous catalysts (including carbon supported Ru, Pt, Ni and Cu) have been employed for GL hydrogenolysis with Ru being considered as the most effective.[10–13]

However, several studies have shown that non-acidic Ru species mainly catalyse the undesired methanation reaction resulting from thermal-induced dehydration to acrolein followed by decomposition to CO and short chain alkanes.[14,15] In comparison, acidic Ru species initialize the first protonation step followed by acid- and thermally-induced consecutive dehydration and subsequent keto–enol tautomerization leading to acetol as reaction intermediate. In the following step, selective hydrogenation to 1,2-PD takes place.[16]

Surface modification of Ru based catalysts either by adding sulphur for poisoning the active Ru sites or by adding another metal is reported in literature to increase the selectivity towards 1,2-Pd.[17] Bimetallic catalysts based on Ru and Fe as a promoter showed superior activity and selectivity for GL hydrogenolysis to PDs compared to monometallic Ru species, especially when supported on carbon nanotubes (CNTs).[18] This can be explained by synergistic effects of the formation of Ru–Fe alloys and the interactions between RuFe bimetallic NPs and iron oxides on CNT surfaces. Moreover, several Cu-based catalysts have been applied for selective 1,2-PD formation. Hereby, mainly Cu chromite,[19] Cu/ZnO[20] as well as Al_2O_3,[21] SiO_2 (ref. 22) and MgO-supported[23] Cu nanoparticles where frequently reported. Additionally, also bimetallic CuAg[24] as well as CuPd[25] catalysts showed good activities for selective glycerol hydrogenolysis. From a mechanistic point of view, the conversion of glycerol to 1,2-PD using Cu as active species can be attributed to a selective cleavage of the C–O bond *via* a hydro-dehydrogenation mechanism proposed by Montassier *et al.*[26] Hereby, a proper balance between hydro-dehydrogenation centres and dehydration centres in Cu-based catalysts is required for a high 1,2-PD selectivity.

[a] *Universität Hamburg, Institut für Technische und Makromolekulare Chemie, Bundesstraße 45, 20146 Hamburg, Germany. E-mail: jakob.albert@chemie.uni-hamburg.de*
[b] *Technische Universität Hamburg, Institut für Kunststoffe und Verbundwerkstoffe, Denickestraße 15, 21073 Hamburg, Germany*

† Electronic supplementary information (ESI) available. See DOI: 10.1039/d1cy01518d

Open Access Article. Published on 20 September 2021. Downloaded on 2/11/2026 9:33:30 AM. This article is licensed under a Creative Commons Attribution-NonCommercial 3.0 Unported Licence.

Open Access Article. Published on 20 September 2021. Downloaded on 2/11/2026 9:33:30 AM.
This article is licensed under a Creative Commons Attribution-NonCommercial 3.0 Unported Licence.

The aim of our study was to find a suitable supported bimetallic catalyst for selective production of 1,2-PD through surface modification of Ru based catalysts. For efficient gas–liquid mass transfer, the micro-, meso- and macrostructure of the catalytic active surface has to be designed in an intelligent way to overcome mass and heat transport limitations by using CNT as catalyst support. We have now developed a superior CNT-supported bimetallic RuCu catalyst that specifically provides a very high selectivity for 1,2-propanediol. In this bimetallic catalyst, Ru is responsible for H_2 spillover which provides active hydrogen to the surface of the Cu nanoparticles and Cu is responsible for C–O cleavage through hydro-dehydrogenating properties.

The carbon nanotubes that were used as support for our new catalyst, are commercially available multi-walled CNT NC7000 by Nanocyl SA., Belgium, which is a nanoparticle powder widely applied in industrial scale CNT-modified materials. The catalysts were synthesised using an improved version of the wet impregnation method described by Asakura *et al.*[18] A detailed description of the synthetic procedure can be found in the ESI.† Table 1 shows the surface properties of the synthesized materials. The total surface area slightly decreases after deposition of the metals on the CNT support. This might be caused by metal particles blocking the pores of CNTs. A similar behaviour was reported before for Ru–Cu supported on CNT.[17] The decrease in surface area was higher in case of Ru_2Cu_1 and Ru_1Cu_2 catalysts, as Cu has a larger particle diameter compared to Ru and Fe. The only exception is for pure Cu which slightly increases the total surface area, possibly by forming separate particles instead of adhering to the CNT surface. The metallic surface area and metal dispersion as well as the active particle diameter were determined by CO-chemisorption. With respect to the metallic surface area, no significant differences between the synthesized materials could be observed.

The dispersion of Ru onto the CNTs is around 50% lower compared to the commercial Ru on carbon. This might be caused by the different surface properties of the CNT as they attract mainly acidic Ru species. Interestingly, the metal dispersion increases when Fe is added to the Ru/CNT catalyst but decreases when Cu is added instead. This correlates with the active particle diameter which increases when Cu is added but decreases when Fe is added. Impregnation of the CNTs with Cu alone results in a very low metal dispersion and large diameter of the active particles. This is due to agglomeration of active Cu during the calcination step in catalyst synthesis.[27] Referring to Ru–Cu impregnation, it is assumed that the Cu adds partly to the Ru particles instead of directly to the CNTs. This results in larger particles with lower dispersion, whereas Fe and Ru independently form small particles on the CNT surface leading to a high dispersion and smaller particle size.

The transmission electron microscopy (TEM) micrographs and energy dispersive X-ray (EDX) mapping analysis of the Ru_2Cu_1-catalyst (Fig. 1) show that the catalysts obtained *via* wetness impregnation of the CNT surface with the catalytically active Ru and Cu nanoparticles retain the multiwall-CNT structure, which confirms the successful immobilization on the CNT support (Fig. 1a). EDX mapping analysis shows that all the chemical elements (C – Fig. 1b, Cu – Fig. 1c, Ru – Fig. 1d) are well represented in the material, which indicates a uniform distribution of the nanoparticles on the CNT surface.

The calcined catalysts were further characterised by powder-X-ray-diffraction (PXRD). In the diffractogram of the pure CNTs (Fig. 2a) only the 111 reflection of graphitic carbon is identifiable at 26°. Moreover, a small broad 111 reflection of orthorhombic Fe_2C is observable at 42°. Orthorhombic RuO_2 (Fig. 2b) is clearly identified by its 111 reflection at 28°, the merged 101 and 011 reflections at 35° and the combined 211 and 121 reflection at 55°, which are present in all three catalyst diffractograms. The diffractogram of Ru_1Cu_2 (Fig. 2c) additionally shows reflections for monoclinic CuO; the 002 and −111 reflections merge with the RuO_2 reflection at 35°, but the combined peak for the 111 and 200 reflections at 39° as well as the −222 reflection at 49° and the merged 022 and −311 reflection at 66° serve as clear identifiers. In the Ru_1Fe_2 diffractogram (Fig. 2d) trigonal Fe_2O_3 is identified by its 104 reflection at 33° and 024 reflection at 49°. Overall the PXRD data (complete PXRD data see ESI,† Fig. S1) confirms the presence of metal-oxide crystallites which are reduced to the respective metals prior to glycerol hydrogenolysis by treating the calcined catalysts in a tube furnace with a mixture of 5% H_2/95% N_2 for 8 h at 550 °C.Hereby, the close interaction of the noble Ru with the

Table 1 Textural properties of catalyst materials

Nominal catalyst composition[a]	Total surface area[b] [$m^2\ g^{-1}$]	Metallic surface area[c] [$m^2\ g^{-1}$ sample]	Metal dispersion[c] [%]	Active particle diameter[c] [nm]
Ru_1Cu_2/CNT	148	2.2	8.3	13.8
Ru_2Cu_1/CNT	164	1.9	8.9	14.0
Cu/CNT	248	1.1	3.4	30.7
Ru_1Fe_2/CNT	171	2.2	25.0	5.3
Ru_2Fe_1/CNT	175	2.3	15.7	8.4
Ru/CNT	182	2.0	11.1	11.9
Ru/C[d]	180	—	19.0	—
CNT	210	—	—	—

[a] Determined by ICP-OES. [b] Measured by N_2-physisoprtion. [c] Determined by CO-chemisorption. [d] Provided by manufacturer.

 This journal is © The Royal Society of Chemistry 2021

Open Access Article. Published on 20 September 2021. Downloaded on 2/11/2026 9:33:30 AM.
This article is licensed under a Creative Commons Attribution-NonCommercial 3.0 Unported Licence.

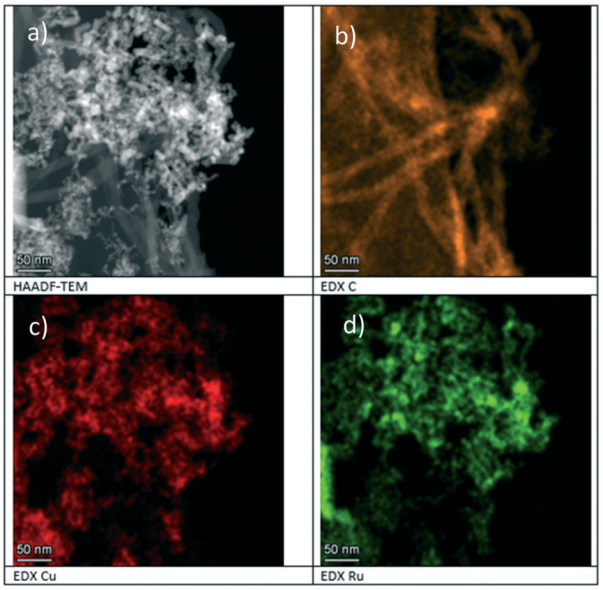

Fig. 1 a) HAADF-TEM image, and EDX elemental mapping images b)–d) of the Ru_2Cu_1 on CNT catalyst. Additional images can be found in the ESI,† Fig. S2–S5.

Fe or Cu inhibits the reduction of Ru and shifted the reduction peaks to higher temperatures. The H_2-TPR profiles of the as-calcined samples with different metal loadings (see ESI,† Fig. S6) show significant differences between the Cu and Fe added Ru/CNT catalysts. Most significantly, the Ru_1Cu_2/CNT catalyst shows the highest degree of reduction supporting the strong intermetallic effect between Cu and Ru. Furthermore, this is clearly shown by the three times higher reduction capacity of Ru_1Cu_2/CNT compared to the other catalysts (Cu, Ru & Ru_1Fe_2 on CNT) with the same metal loading. This strong surface interaction between Cu and Ru metals was also previously reported using XPS studies by Jiang *et al.*[28] XPS showed shifts in binding energies of the active metal species and an electron transfer from Ru to Cu. This electron transfer leads to an inhibition of the undesired methanation reaction catalysed by Ru through C–C-bond cleavage. Therefore, the Cu-catalysed cleavage of the C–O bond, leading to the preferred 1,2-PD, is promoted.

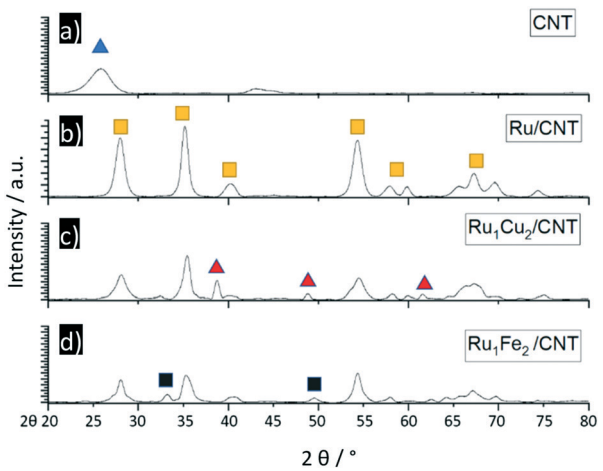

Fig. 2 PXRD-diffractograms of selected catalysts a)–d), measured with Cu-Kα radiation, the blue triangle indicates reflexes for graphitic carbon, the yellow square for RuO_2, the red triangle for CuO and the black square for Fe_2O_3.

The predominant product in the catalytic hydrogenolysis experiments was the desired 1,2-propanediol (1,2-PD) with up to 93% selectivity for the bimetallic Ru_1Cu_2/CNT catalyst. Moreover, ethylene glycol (EG) was formed as the main liquid byproduct from initial C–C-bond cleavage with up to 21% using Fe/CNT. Other products in liquid phase were identified as hydroxyacetone (HA), propionic acid (PA) as well as iso- and *n*-propanol (iso-Pr, *n*-Pr), ethanol (EtOH), and methanol (MeOH). In the gas phase, mainly methane (up to 28% for Ru/C) as well as small amounts of ethane, propane and CO_2 were found. The formation of CO_2 in an otherwise reductive environment can be explained by an aqueous phase reforming mechanism.[29] Table 2 gives an overview of product selectivity and conversion for each catalyst. Moreover, the carbon balance could be closed to >90% for all catalytic runs showing the high accuracy of the used equipment. HPLC and GC were used to determine the mass balance and the product yields in the liquid and gaseous phases respectively as illustrated in the ESI.†

Control experiments without catalyst show that no glycerol conversion occurs by pure thermal activation. The CNTs themselves show almost no catalytic activity, a minimal conversion was recorded, which might be caused by metallic impurities like Al and Fe stemming from the CNT synthesis. (Characterisation of the CNTs is provided in the ESI†). The comparison between the commercial Ru on C catalyst and Ru on CNT shows a huge improvement in the selectivity for 1,2-PD from 21 to around 52% accompanied by an increased glycerol conversion form 46% up to 74%, which can only be attributed to the beneficial interplay of the CNT support and the deposited Ru particles. We speculate that aside from a possible promoting effect of the metal impurities (mainly Al) in the CNTs, the CNT surface promotes a beneficial orientation of the metal crystallites on the surface.

The introduction of Fe has been reported to greatly enhance the performance of the Ru catalyst.[18] However in our experiments, the addition of Fe did neither improve the conversion nor the selectivity for 1,2-PD significantly compared to pure Ru on CNT. Nevertheless, it is noteworthy that a larger Fe content (Ru_1Fe_2 on CNT) appears to limit the conversion (49% compared to 78% for Ru_2Fe_1 on CNT) while at the same time slightly increases the selectivity for 1,2-PD (59.5% *vs.* 44.8%). This might be due to the more efficient C–O bond cleavage caused by the synergistic effects of the resulting RuFe nanoparticles. As stated above, Cu based catalysts have previously shown a good selectivity for the formation of propanediols from glycerol.[19–23]

A test with pure Cu on CNT shows a very high selectivity (>99%) for 1,2-PD, which is however accompanied by a very low activity (conversion of only 4%).

Open Access Article. Published on 20 September 2021. Downloaded on 2/11/2026 9:33:30 AM.
This article is licensed under a Creative Commons Attribution-NonCommercial 3.0 Unported Licence.

Table 2 Glycerol hydrogenolysis using different catalysts. Results from Ru/C and without catalyst are averaged over 7 experiments, results for Fe/CNT were taken from literature[17]

Catalyst-composition	Conversion [%]	Selectivity [%]												Carbon balance [%]
		1,2-PD	EG	HA	PA	*i*-Pr	*n*-Pr	EtOH	MeOH	CH_4	C_2H_6	C_3H_8	CO_2	
Ru_1Cu_2/CNT	18.0	**93.4**	4.1	0	0.7	0	1.0	0	0	2.5	<1	<1	<0.5	100
Ru_2Cu_1/CNT	21.2	**83.6**	5.0	0	2.1	0	1.5	0	0	3.5	<1	<1	<1	99
Cu/CNT	4.2	**>99**	2.1	<1	2.1	0	0	0	0	0	0	0	1.9	100
Ru_1Fe_2/CNT	49.1	**59.5**	9.9	0	4.5	<1	3.8	1.2	0	8.6	1.0	1.8	<1	96
Ru_2Fe_1/CNT	78.2	**44.8**	6.4	1.5	8.4	1.5	2.0	1.5	0	8.9	1.7	2.3	2.5	86
Fe/CNT[17]	2.8	**64.3**	20.9	n.d.	n.d.	n.d.	n.d.	n.d.	n.d.	2.1	n.d.	n.d.	n.d.	n.d.
Ru/CNT	74.4	**51.8**	6.7	1.8	8.2	1.5	3.1	1.8	0	10.5	2.4	3.7	2.3	96
Ru/C	45.9	**20.5**	13.2	5.4	0	0	0	<1	1.3	27.7	3.6	2.1	2.4	89
CNT	0.3	**0**	0	0	0	0	0	0	0	4.5	0	0	0	100
No cat.	0	—	—	—	—	—	—	—	—	—	—	—	—	100

Reaction conditions: 2 g glycerol (10 mL of 20 wt% aqueous solution); catalyst amount = 200 mg; H_2 pressure = 5.0 MPa; T = 200 °C; stirring speed = 1000 rpm. t = 20 h.

As indicated above, pure Cu seems to form nanoparticles separately from the CNTs and therefore does not benefit from the promoting effect of the CNT support. The optimised catalyst system therefore contains both, Ru and Cu and provides very high selectivity for the desired product (up to 93%) as well as moderate catalyst activity (up to 21%). We have observed the highest selectivity with a catalyst of the composition 5% Ru_1Cu_2 on CNT (93.4%) while the catalyst with the composition 5% Ru_2Cu_1 on CNT provides a marginally higher conversion rate (21%) with a slightly lower selectivity for 1,2-PD (84%). Additionally, the active particle size for the pure Cu catalyst is comparatively large with around 31 nm while the metallic surface area is the lowest with only 1.1 m^2 g^{-1} sample (Table 1). In contrast, the bimetallic Ru–Cu catalysts have well distributed metal nanocrystallites (confirmed by TEM pictures as well as EDX elemental mapping) with a metallic surface area similar to the bimetallic Ru–Fe catalysts of around 2 m^2 g^{-1} sample. The larger active particle size and thereby lower dispersion of the Ru–Cu catalysts are probably the reason for the lower activity (conversion). The direct correlation between Cu content and selectivity for 1,2-PD indicates that the preference for C–O bond cleavage is an inherent property of the Cu particles. Future improvements in the catalyst synthesis procedure might improve the particle size and dispersion. Moreover, in combination with optimisation of the reaction parameters, high conversion can likely be achieved while maintaining the very high selectivity to the desired 1,2-PD.

To sum up, adding Cu to Ru nanoparticles dispersed on a CNT support by employing an improved wetness impregnation method significantly enhances the reducibility and modified the surface of the resulting Ru–Cu species. Hereby, the chemical composition of the resulting bimetallic Ru–Cu catalyst as well as the surface interaction between Cu and Ru led to a promoting effect resulting in a preference for C–O bond cleavage promoted by Cu over C–C bond cleavage catalysed by small Ru nanoparticles. By employing this catalyst for the hydrogenolysis of glycerol a superior 1,2-PD selectivity of 93.4% was achieved.

Conflicts of interest

There are no conflicts of interest to declare.

Notes and references

1 D. Voß, H. Pickel and J. Albert, *ACS Sustainable Chem. Eng.*, 2019, **7**, 9754–9762.
2 S. Sandesh, P. Manjunathan, A. B. Halgeri and G. V. Shanbhag, *RSC Adv.*, 2015, **5**, 104354–104362.
3 B. N. Zope, D. D. Hibbitts, M. Neurock and R. J. Davis, *Science*, 2010, **330**, 74–78.
4 A. Corma, S. Iborra and A. Velty, *Chem. Rev.*, 2007, **107**, 2411–2502.
5 D. Sun, Y. Yamada, S. Sato and W. Ueda, *Appl. Catal., B*, 2016, **193**, 75–92.
6 A. M. Ruppert, K. Weinberg and R. Palkovits, *Angew. Chem., Int. Ed.*, 2012, **51**, 2564–2601.
7 D. M. Alonso, S. G. Wettstein and J. A. Dumesic, *Chem. Soc. Rev.*, 2012, **41**, 8075–8098.
8 Y. Wang, J. Zhou and X. Guo, *RSC Adv.*, 2015, **5**, 74611–74628.
9 J. ten Dam and U. Hanefeld, *ChemSusChem*, 2011, **4**, 1017–1034.
10 T. Miyazawa, Y. Kusunoki, K. Kunimori and K. Tomishige, *J. Catal.*, 2006, **240**, 213–221.
11 W. Oberhauser, C. Evangelisti, R. P. Jumde, R. Psaro, F. Vizza, M. Bevilacqua, J. Filippi, B. F. Machado and P. Serp, *J. Catal.*, 2015, **325**, 111–117.
12 A. Modvig, C. Kumpidet, A. Riisager and J. Albert, *Materials*, 2019, **12**, 2175.
13 H. Zhao, L. Zheng, X. Li, P. Chen and Z. Hou, *Catal. Today*, 2020, **355**, 84–95.
14 Y. Nakagawa and K. Tomishige, *Catal. Sci. Technol.*, 2011, **1**, 179–190.
15 E. Maris and R. Davis, *J. Catal.*, 2007, **249**, 328–337.
16 Z. Huang, F. Cui, H. Kang, J. Chen and C. Xia, *Appl. Catal., A*, 2009, **366**, 288–298.
17 Z. Wu, Y. Mao, X. Wang and M. Zhang, *Green Chem.*, 2011, **13**, 1311–1316.

 This journal is © The Royal Society of Chemistry 2021

Open Access Article. Published on 20 September 2021. Downloaded on 2/11/2026 9:33:30 AM.
This article is licensed under a Creative Commons Attribution-NonCommercial 3.0 Unported Licence.

18 B. Li, J. Wang, Y. Yuan, H. Ariga, S. Takakusagi and K. Asakura, *ACS Catal.*, 2011, **1**, 1521–1528.
19 C. Wang, H. Jiang, C. Chen, R. Chen and W. Xing, *Chem. Eng. J.*, 2015, **264**, 344–350.
20 Y. Du, C. Wang, H. Jiang, C. Chen and R. Chen, *J. Ind. Eng. Chem.*, 2016, **35**, 262–267.
21 C. Liu, C. Zhang, S. Hao, S. Sun, K. Liu, J. Xu, Y. Zhu and Y. Li, *Catal. Today*, 2016, **261**, 116–127.
22 S. Zhu, X. Gao, Y. Zhu, Y. Zhu, H. Zheng and Y. Li, *J. Catal.*, 2013, **303**, 70–79.
23 M. Balaraju, K. Jagadeeswaraiah, P. S. S. Prasad and N. Lingaiah, *Catal. Sci. Technol.*, 2012, **2**, 1967–1976.
24 J. Zhou, L. Guo, X. Guo, J. Mao and S. Zhang, *Green Chem.*, 2010, **12**, 1835–1843.
25 A. N. Ardila, M. A. Sánchez-Castillo, T. A. Zepeda, A. L. Villa and G. A. Fuentes, *Appl. Catal., B*, 2017, **219**, 658–671.
26 C. Montassier, D. Giraud and J. Barbier, in *Studies in Surface Science and Catalysis*, Elsevier, 1988, vol. 41, pp. 165–170.
27 S. Zhu, X. Gao, Y. Zhu, W. Fan, J. Wang and Y. Li, *Catal. Sci. Technol.*, 2015, **5**, 1169–1180.
28 T. Jiang, Y. Zhou, S. Liang, H. Liu and B. Han, *Green Chem.*, 2009, **11**, 1000–1006.
29 M. Checa, S. Nogales-Delgado, V. Montes and J. M. Encinar, *Catalysts*, 2020, **10**, 1279.